

Experimental Study to Understand the Effect of Residual Stress and Applied Load on Creep Relaxation



Anilkumar Shirahatti

Abstract In structural integrity analysis of components operating at high temperature, it is important to understand whether the presence of residual stresses lead to failure [1]. Accurate prediction of the creep crack initiation is needed in structural integrity assessments of components. General assessment of structures uses the experimental data obtained from laboratory test specimens subjected to either displacement or load tests but in actual operating condition, components are subjected to both inherent residual stresses and applied load. In the current research work, two test rigs are designed and tests are performed to understand the effects of EFU, long-range residual stress and external applied load on creep behaviour of 316H stainless steel. Results obtained show that, for the same total initial reference stress, the time for crack to grow is lower in the case of mixed loading conditions compared to load-controlled tests. The longer crack growth times are a consequence of the relaxation and redistribution of the residual loads in the structure. The initiation time is also a function of the elastic follow-up.

Keywords Crack growth · Residual stress · Creep · Elastic follow-up

1 Introduction

A nuclear power station has a large amount of welds, viz. nearly 2000 welds are present in large bore steam pipe work [2, 3]. Welded joints are particularly vulnerable to plant degradation and material ageing. Welded engineering components operating at high temperature will be subjected to the combinations of residual stress and applied load. When components are subjected to the applied load, it is usually termed as to induce primary stresses or load-controlled stress, while residual stresses present in the components are often considered as secondary stresses or a displacement-controlled stress. When components are working under high temperature condition, residual stresses are expected to relax with respect to time [4, 5]. The interaction will

A. Shirahatti (✉)

Department of Mechanical Engineering, Jain College of Engineering, Belagavi, India
e-mail: anilshirahatti@gmail.com

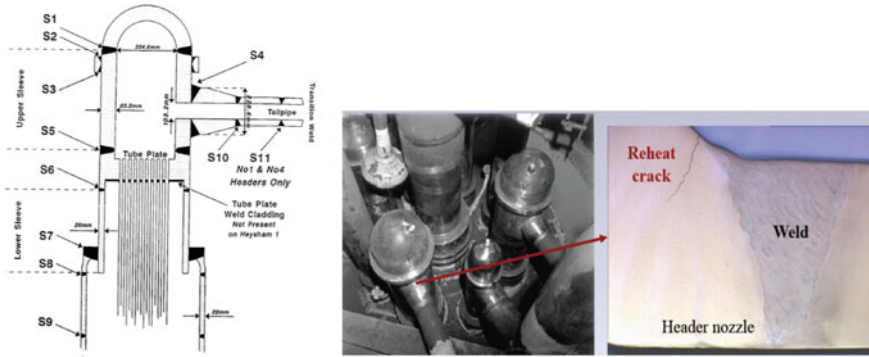


Fig. 1 Superheater header: type 316H austenitic stainless steel thick section weldments [5]

become more complex, if there is a combination of both residual stress and applied load. Weld residual stresses are created by misfit strains and as such essentially represent displacement-controlled boundary conditions. Usually, welded components are then subjected to an externally applied load. The subsequent deformation of the welded sample can be viewed as being associated with combined boundary conditions, i.e. combined displacement and load-controlled situations. Figure 1 shows thick section weldments of 316H austenitic stainless steel in the superheater header. Crack initiation was observed in welded components operating at high temperature due to the presence of combined weld residual stress and applied stress [6].

In the life assessment of structural components, residual stress plays an important role. Residual stresses may arise in the components or structures as a consequence of the manufacturing process adopted and final fabrication [7, 8]. If residual stress is tensile in nature, then it can combine with applied loads and lead to failure of the component at a load seems to safer from design point of view. Thus, for accurate assessments of components, a quantitative understanding of behaviour of residual stresses with applied load is needed.

In the case of creep crack initiation and growth, many experiments are carried out using standard laboratory-scale creep test specimens tested under load-controlled [9, 10] and occasionally under displacement-controlled conditions [11]. However, structures are subjected to stresses that arise from a combination of residual and applied stresses. The relaxation of residual stress in one location is compensated by changes in residual stress distribution in other locations so as to retain equilibrium, i.e. components are often subjected to combined displacement- and load-controlled conditions. Furthermore, it is now known [2, 12–18] that, depending on the stiffness of the structure, relaxation of the residual stress can be associated with elastic follow-up.

The purpose of this paper is to illustrate a three-bar test rig that was designed [5, 7] to introduce the combinations of residual and applied stresses into a compact tension C(T) specimen. The residual stresses can be induced in a controlled manner and can be characterized easily. Tests are performed to understand the effect of residual stresses and applied load on creep crack initiation and relaxation.

2 Test Rig Design

The concept of test rig is illustrated in Fig. 2. The test rig was designed such that in a controlled manner residual stresses can be induced and will also have further provision to apply external load to the complete test rig. The middle bar in test rig consists of C(T) specimen and other part of bar with stiffness X_{sp} and X_m respectively. There are two bars having a stiffness X_{out} each. An initial tensile residual stress is induced in middle bar using initial misfit Y , which is further balanced by combine compressive forces acting outer bars. Once known, residual force is induced and equilibrium is reached, an external load is applied to the complete test rig. More details about the design are given in [5, 7].

Stiffness of the specimen relative to the stiffness of the other parts of middle bar and outer bars will decide the value of elastic follow-up of the structure, Z . The overall EFU value, Z can be found using the Eq. (1).

$$Z = Z_s Z_{eff} \tag{1}$$

where

$$Z_s = \left(\frac{1 + \beta}{\beta} \right), Z_{eff} = \left(\frac{1 + \alpha_{eff}}{\alpha_{eff}} \right), \frac{1}{X_{eff}} = \frac{1}{X_{sp}} + \frac{1}{X_m}, \alpha_{eff} = \frac{2X_{out}}{X_{eff}}, \beta = \frac{X_m}{X_{sp}}$$

A detailed derivation of Eq. (1) is explained in [7]. As per R5 Standards [4], the value of overall EFU Z greater than 5 represents load-controlled behaviour, while a value near to 1 gives displacement-controlled behaviour. Hence, it was decided to design and manufacture two test rigs, which fulfill R5 Standard criteria. Figure 3 shows the detailed schematic diagram of test rig and more details about design and manufacturing are given in [7].

Thermocouples are connected to measure the specimen temperature, room temperature and strain gauge temperature. A potential drop system is used to measure the crack initiation and growth, while capacitance gauge mounted on C(T) specimen

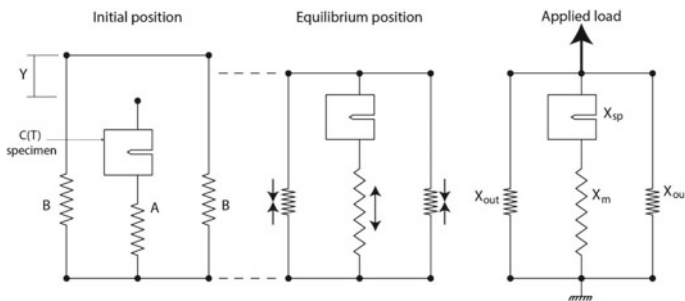


Fig. 2 Concept of three-bar structure

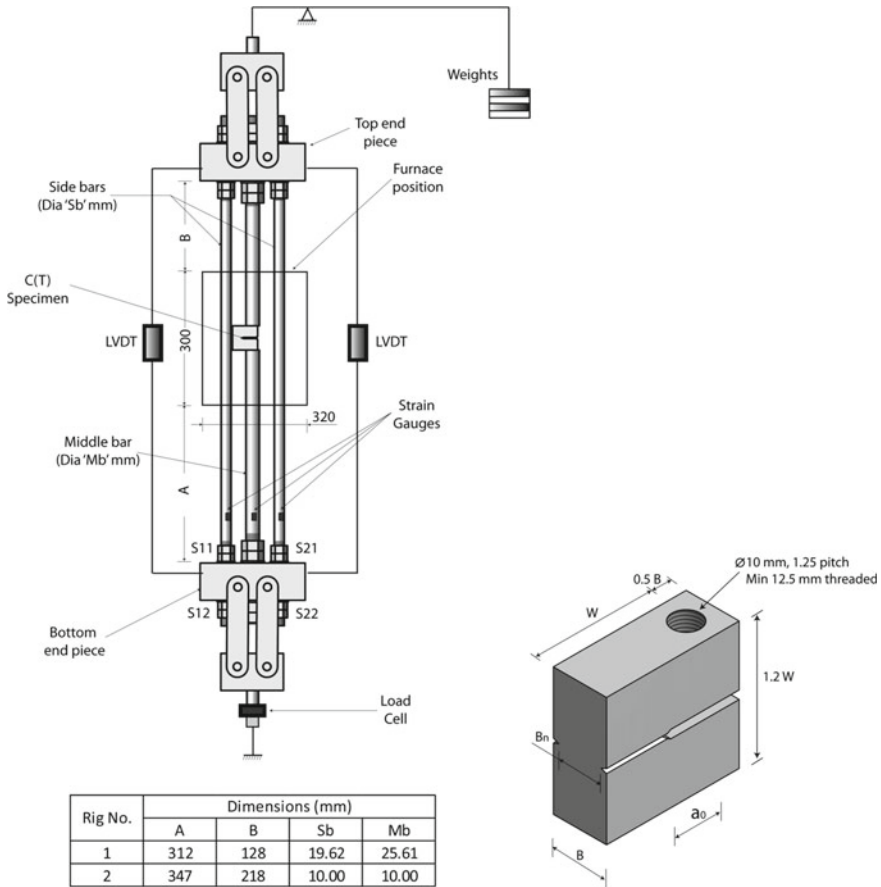


Fig. 3 Three-bar test rig

is used to measure load line displacement. Two LVDTs are mounted at side to measure the overall displacement of the test rig. The external load is applied via a lever arm arrangement.

3 Preparation of Test Specimen

The test specimens were manufactured according to ASTM 1457 [19] from ex-service Type 316H stainless steel supplied by EDF Energy. A screw-fitting arrangement (see Fig. 3) rather than pins were adopted to provide an accurate measurement of stiffness. A 2-mm pre-crack was introduced using 0.1-mm EDM wire such that crack length to width ratio of 0.5 is maintained. Tables 1 and 2 give details of C(T) specimen and material composition of the test specimens.

Table 1 Details of C(T) specimens

Rig No.	Test ID	W (mm)	B (mm)	B _n (mm)	a ₀ (mm)
Load control	LC-01	38.07	19.04	15.36	19.36
Low EFU: Z = 2.15	MX-01	38.05	19.03	15.38	19.59
High EFU: Z = 7.34	MX-02	37.83	19.04	15.36	19.59

4 Introduction of Residual Stress in the Structure

First, in the C(T) specimen, middle bars were connected to top and bottom end pieces. The outer bars were then connected to top end piece and they have provision to move freely through the clearance holes provided at the bottom end piece. Instruments, viz. strain gauges, LVDTs, thermocouples, were connected to data logger and furnace was switched on to achieve a temperature of 550 °C for the C(T) specimen. When C(T) specimen reached a stable temperature as per ASTM standards, nuts S21 and S11 (shown in Fig. 3) were screwed down, so that the both the end pieces were forced apart. Under the equilibrium conditions, this results in tensile load in middle bar and balancing compressive forces in outer bars. Force acting in bars can be easily found by strain gauges mounted on them. Finally, when the desired amount of residual force was introduced into the structure, nuts S22 and S12 on side bars were fixed and the entire assembly was then subjected to an applied load.

5 Creep Crack Tests

In total, three creep crack growth tests were performed and more details are given in Table 3. LC-01 test is the load-controlled test performed on conventional lever arm test rig. Additionally, one test each was performed on three-bar test rig. The initial total reference stress on three-bar test rig was selected such a way that it matches with the load control test. However, the combination of applied and initial residual stresses was different depending on the ease of inducing residual stress and to avoid any twisting or bending. During the tests, the applied load was monitored using the load cell shown in Fig. 3. The combined residual and applied forces in the middle and outer bars were measured using the strain gauges.

Table 3 provides the details of the test conditions together with calculated reference stresses. The tests were continued to permit sufficient changes in potential drop to be measured. The tests were then stopped, specimen were broken open and final crack lengths measured.

The reference stress in Table 3 was determined from [4, 20].

$$\sigma_{ref} = \frac{P}{WB_n n_L} \tag{2}$$

Table 2 Chemical composition of the specimen made of 316H stainless steel

Chemical	P	Cr	Mo	C	S	N	Si	Al	V	W	Mn	Ti	Cu	W	Co
Weight (%)	0.02	17.1	2.38	0.04	0.014	11	0.29	<0.005	0.02	0.042	1.49	0.013	0.09	0.042	0.09

Table 3 Summary of tests

Details/Specimens	LC-01	MX-01 (Z = 2.15)	MX-02 (Z = 7.34)
<i>Initial condition (Start of Tests)</i>			
Initial residual force (kN)	–	8.91	6.36
Initial residual reference stress (MPa)	–	183	130
Applied load (kN)	12.46 kN	2.79	5.43
Applied reference stress (MPa)	240 MPa	57	110
Total initial reference stress (MPa)	240 MPa	240 (223)	240
<i>Final condition (End of Tests)</i>			
Total load (kN)	12.46	5.27	10.97
Total reference stress (MPa)	240 MPa	108	224
Final crack growth (mm)	0.882	0.030	0.169
Test duration (hrs)	1508	4882.4	4229

where n_L is a normalized limit load function given by

$$n_L = \sqrt{(1 + \gamma)(1 + \gamma(a/W)^2)} - (1 + \gamma(a/W)) \text{ with } \gamma = 2/\sqrt{3}$$

6 Results and Discussion

In tests MX-01 and MX-02, a residual force of 8.91 kN and 6.36 kN was introduced into the C(T) specimen, respectively. In both the tests, residual force acting in the middle bar was approximately equal to the summation of the compressive forces acting in side bars. The load versus load line displacement behaviour of all specimens is shown in Fig. 4. Initial residual forces acting on test specimens MX-02 and MX-01 are represented by points A2 and B2, respectively. The curve A2–A3 and B2–B3 represents the application of applied loads, while A3–A4 and B3–B4 corresponds to the relaxation of load acting on the specimen with respect to time. Figure 5 shows the load line displacement for all the tests.

The variation of forces in all bars with respective to time for both rigs is shown in Figs. 6 and 7. It is evident that when external load was applied in case of MX-01, C(T) specimen on test rig 1 with $Z = 2.15$, relaxation of load from 11.7 to 10.87 kN took place. Also, there was an additional plastic deformation that took place in specimen when compared to conventional load control test. The MX-02 C(T) specimen test on test rig 2 with $Z = 7.34$ showed less additional plastic deformation during external loading. This phenomenon is due to the higher EFU value in rig 2.

During the creep process, it was found that the total load was relaxed in both the specimens and as expected the rate of relaxation is high for MX-01 than MX-02.

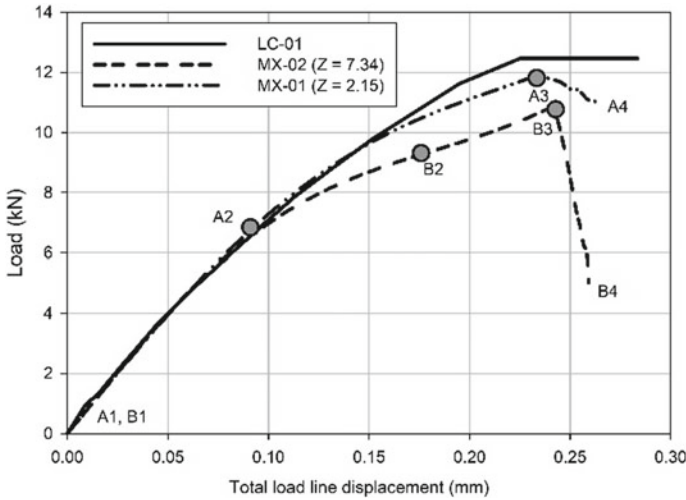


Fig. 4 Load versus total load line displacement for C(T) specimens

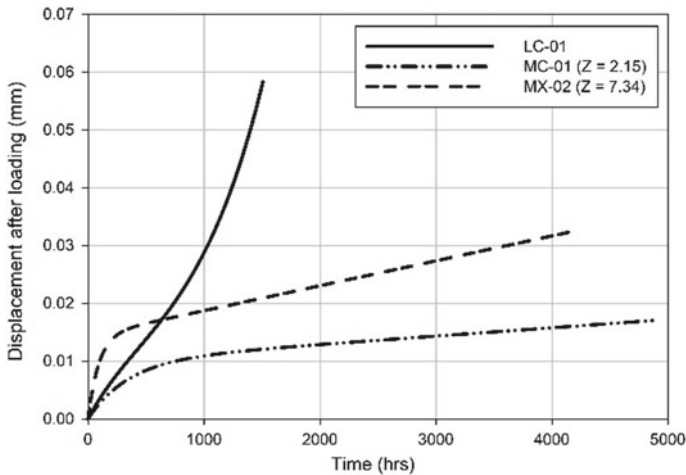


Fig. 5 Comparison of displacements after loading

In case of MX-01, after 4883 h of creep, the initial induced residual stress was relaxed from 183 MPa (8.91 kN) to 51 MPa (2.48 kN). While in case of specimen MX-02, after 4229 h, the initial induced residual stress was relaxed from 130 MPa (6.36 kN) to 113 MPa (5.54 kN). It is observed that the stiffness of the C(T) specimen was decreasing due to creep and crack growth and hence with respect to time a greater portion of the applied load was carried by the outer bars. The slope of relaxation curves A3–A4 and B3–B4 in Fig. 4 is dependent on the relative stiffness of C(T) specimen and other components of the test rig, and which in turn corresponds to

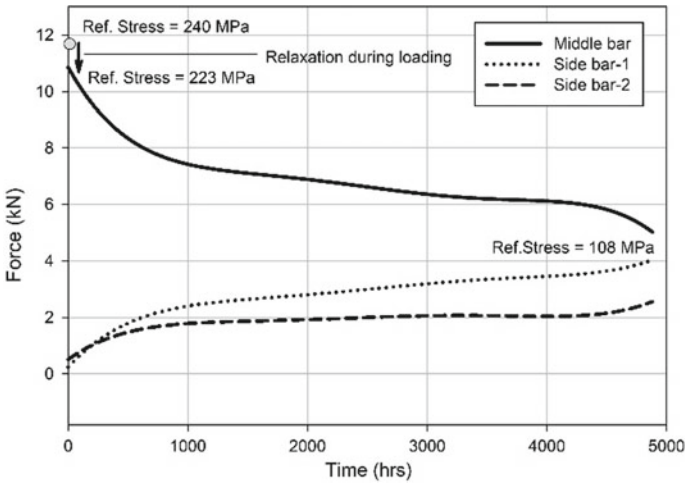


Fig. 6 Variation of force in all bars with time (MX-01)

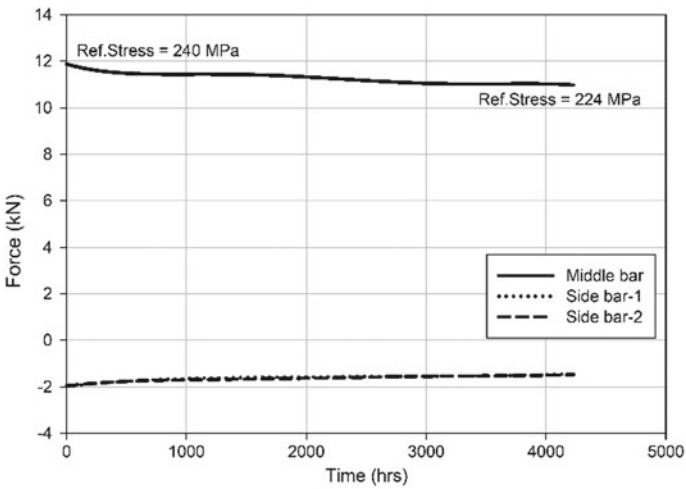


Fig. 7 Variation of force in all bars with time (MX-02)

EFU values associated with test rigs. It can be concluded that rig with higher EFU considers the residual load as load control, while the test rig with lower EFU considers it as displacement control.

Figures 5 and 8 show the measure crack load line displacement and crack growth, respectively, for LC-01, MX-01 and MX-02. It is evident that for the same total initial reference stress, the creep load line displacement was greater for MX-02 than MX-01. Also, crack initiation of 0.03 mm occurred much early in case of MX-02 than MX-01, but both were much later than LC-01.

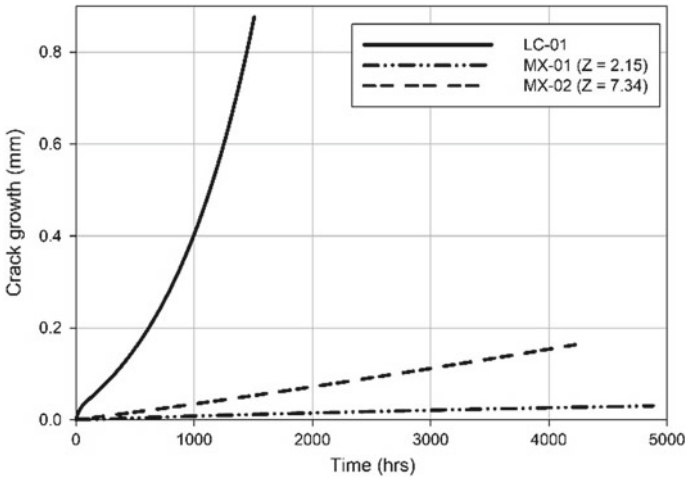


Fig. 8 Comparison of crack growth

The crack initiation times for the various tests are shown in Fig. 9, where, together with the tests performed and explained in the current paper additional tests performed in [6, 7, 9] are also reported. It reveals that, while the initial reference stress was the same for tests LC-01, MX-01 and MX-02, creep crack initiation times were significantly different. For a crack length of 0.03 mm in load control case, it took 52.46 h, while for low and high EFU tests, it took 4882.4 h and 873.9 h, respectively. Rig with low EFU will contribute for more load relaxation and redistribution than high EFU and thus it will lead to an increase in creep crack initiation time. Figure 10

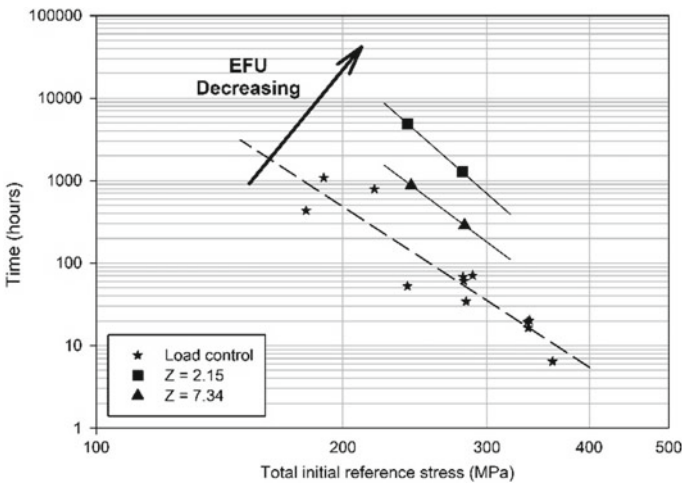


Fig. 9 Comparison of time for cracks to grow 0.03 mm

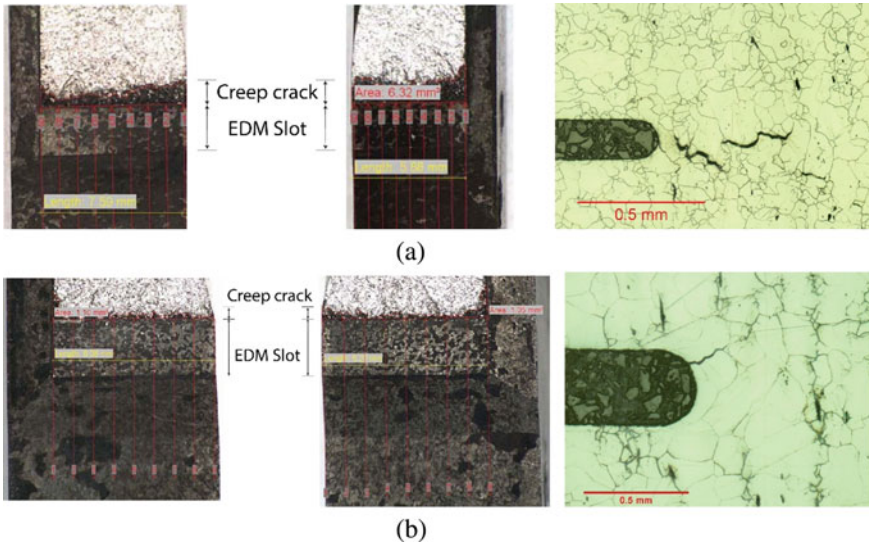


Fig. 10 Comparison of Crack growth and Micrograph of specimen **a** LC-01, **b** MX-02

shows the crack growth and micrographs of the specimen LC-01 and MX-02. All the creep tests appeared to fail in an intergranular crack growth and to consist mainly of wedge cracking. More detailed micrographic analysis is given in [7].

7 Conclusion

Structural integrity analysis of components is based on conventional laboratory load-controlled or displacement-controlled tests, but in actual working condition, they are subjected to combination of residual stress and applied load. This in turn represents mixed load conditions. In the current paper, two test rigs with EFU near 2 and 7 were developed. The rigs are designed on the concept of three-bar structure, in which residual stresses can be introduced in a controlled manner. The results obtained shows that even though the initial reference stresses were the same for mixed and load-controlled test, the initiation times were longer in mixed boundary condition test. Also, it is found that with initiation times were high for lower values of elastic follow-up test rig. The longer initiation times were due to the relaxation and redistribution of the residual and applied loads in the structure.

Acknowledgements The author gratefully acknowledges EDF Energy, United Kingdom for the financial support for this work and research facility provided by the University of Bristol, United Kingdom. The author also acknowledges Dr. David Dean and Mr. Mike Spindler of Structural Integrity Group at EDF Energy, for lending their expertise and advice.

References

1. Shirahatti AM, Smith DJ (2015) The effects of long-range residual stress, elastic follow-up and applied load on creep crack incubation and material toughness. *J Strain Anal Eng Des*, JSA Golden Issue, July 2015, pp 1–15
2. Robinson EL (1955) Steam piping design to minimize creep concentration. *Trans ASME* 77:1147–1162
3. Shirahatti AM, Truman CE, Smith DJ (2013) Experiments to determine the influence of residual stress and elastic follow-up on creep crack initiation. In: *Proceedings of the ASME 2013 pressure vessels & piping conference*, Paris, France
4. British Energy Generation Ltd. (2003) Assessment procedure for the high temperature response of structures. R5 Standards, Issue 3
5. Shirahatti AM, Smith DJ (2019) A novel creep test rig to study the effects of long-range residual stress, elastic follow-up and applied load. *J Braz Soc Mech Sci Eng* 41(230):1–12
6. Bouchard PJ, Withers PJ, McDonald SA, Heenan RK (2004) Quantification of creep cavitation damage around a crack in a stainless steel pressure vessel. *Acta Mater* 52(1):23–34
7. Shirahatti AM (2014) A novel test rig to study the effects of elastic follow-up, long range residual stress and applied load on creep crack initiation. PhD thesis, University of Bristol, United Kingdom
8. Kapadia P, Davies CM, Dean DW, Nikbin KM (2012) Numerical simulation of residual stresses induced in compact tension specimens using electron beam welding. In: *Proceedings of the ASME 2012 pressure vessels & piping conference*, Toronto, Ontario, Canada
9. Dean DW, Gladwin DN (2007) Creep crack growth behavior of Type 316H steels and proposed modifications to standard testing and analysis methods. *Int J Press Vessels Pip* 84:378–395
10. Fookes AJ (2003) Assessment of crack growth in steels at high temperature. PhD thesis, Bristol University, United Kingdom
11. Gladwin DN, Allport L, January (2010) The constant static displacement controlled creep crack growth response of 316H stainless steel header material. Technical report, British Energy Generation Ltd., Report No. E/EAN/BDBB/0024/AGR/06
12. Hadidi-Moud S, Smith DJ (2008) Use of elastic follow-up in integrity assessment of structures. In: *Proceedings of the ASME 2008 pressure vessels & piping conference*, Chicago, Illinois, USA
13. Aird CJ, Mahmoudi AH, Mirzaee Sisan A, Truman CE, Smith DJ (2006) Generating well defined residual stresses in laboratory specimens. In: *Proceedings of the ASME 2006 pressure vessels & piping conference*, Vancouver, BC, Canada
14. Shirahatti AM, Wang Y, Truman CE, Smith DJ (2013) A new method of introducing long range residual stresses to study creep crack initiation. In: *13th international conference on fracture*, Beijing, China
15. Hossain S, Truman CE, Smith DJ (2011) Generation of residual stress and plastic strain in a fracture mechanics specimen to study the formation of creep damage in type 316 stainless steel. *Fatigue Fract Eng Mater Struct* 34:654–666
16. Wang YQ, Coules HE, Truman CE, Smith DJ (2018) Effect of elastic follow-up and ageing on the creep of an austenitic stainless steel. *Int J Solids Struct* 135:219–232
17. Kapadia P, Davies CM, Dean DW, Nikbin KM (2015) Assessment of creep crack growth due to assessment of creep crack growth due to secondary and combined loading. *Transactions, SMIRT-23*, Manchester, United Kingdom
18. Khayat-zadeh S, Tanner D, Truman CE, Flewitt P, Smith DJ (2017) Influence of thermal ageing on the creep of a P92 martensitic steel. *Mater Sci Eng A* 708:544–555
19. American Society for Testing and Materials (2000) Standard test method for measurement of creep crack growth rates in metals. ASTM E1457-00
20. R6 Revision 4 Amendment 8 (2010) Assessment of the integrity of structures containing defects. BEGL procedure